AIAA JOURNAL
Vol. 41, No. 10, October 2003

Deterministic and Reliability-Based Optimization of Composite Laminates for Cryogenic Environments

Xueyong Qu* and Raphael T. Haftka†
University of Florida, Gainesville, Florida 32611
Satchi Venkataraman‡
San Diego State University, San Diego, California 92182-1308
and
Theodore F. Johnson§
NASA Langley Research Center, Hampton, Virginia 23681-2199

Designs of composite laminates are investigated for hydrogen tanks in cryogenic environments. Large residual strains, which can develop due to thermal mismatch between matrix and fibers, result in matrix cracking at cryogenic temperatures and increase hydrogen leakage through the tank wall. To reduce thermal mismatch, ply angles need to be close to each other, but this leads to a substantial weight increase under biaxial loading. First deterministic optimization is used to investigate possible weight reduction measures. Reducing axial loads on walls by auxiliary stiffening mechanisms led to significant weight reduction. Reliability-based optimizations were performed to identify the uncertainties in composite material properties with the largest influences on the optimum design. Then measures for reducing uncertainty in important parameters are examined. The results indicate that the most effective measure for reducing thickness is quality control.

Nomenclature

E, σ, CV	=	mean value, standard deviation, and coefficient of variation (σ/E) of the random variables
E_1, E_2, G_{12}	=	elastic modulus along and transverse to fiber direction and shear modulus of a composite ply
h	=	total laminate thickness
T_{zero}	=	stress-free temperature
t_1, t_2	=	thickness of plies with angles θ_1 and θ_2, respectively
α_1, α_2	=	coefficient of thermal expansion along and transverse to fiber direction
$\varepsilon_1, \varepsilon_2, \gamma_{12}$	=	strains along and transverse to fiber direction and shear strain of a composite ply
$\theta, \theta_1, \theta_2$	=	ply orientation angles
μ_{12}	=	major Poisson ratio of a composite ply

Subscripts

l	=	lower limit
u	=	upper limit

Introduction

THE use of composite materials in liquid hydrogen tanks at cryogenic temperatures involves many challenges. Large thermal strains develop due to the mismatch of the thermal expansion coefficients in the fiber and transverse directions. The residual thermal strains may result in matrix cracking, which reduces the stiffness and strength of the laminate and may initiate delamination failure. Another potentially detrimental effect of matrix cracking in hydrogen tanks can also cause hydrogen leakage through the wall of the tank. Park and McManus[1] proposed a micromechanical model of laminate cracking based on fracture mechanics and verified the model by experiments. Kwon and Berner[2] studied matrix damage of cross-ply laminates by combining a simplified micromechanics model with finite element analysis and showed that the prediction of damage is improved substantially with the incorporation of residual stresses. Aoki et al.[3] modeled and successfully predicted the leakage through matrix cracks.

To reduce matrix cracking, laminates designed for cryogenic environments need to have smaller angles between plies. For example, ±25-deg laminates have been used for such applications.[4] These types of laminates, however, do not efficiently carry the biaxial hoop and axial stresses due to pressure.

The objective of this paper is to investigate available options for minimizing the increase in thickness required to carry both mechanical and thermal residual strains. Deterministic optimizations were performed to investigate the use of auxiliary stiffening solutions that reduce the axial mechanical load on the tank wall laminate. Furthermore, reliability-based optimization was used to investigate options for weight reduction by controlling material variability.

The composite material used was the IM600/133 graphite–epoxy material system, tested by Aoki et al.[3] at various temperatures, from 356 to −452.2°F (180 to −269°C), with mechanical tensile loads. They showed that the fracture toughness of the material increased at lower temperatures; however, the increased strain energy due to the mismatch in the thermal expansion coefficients also increased the critical energy release rate. They also applied the micromechanics model proposed by Park and McManus[1] for predicting microcracking and showed good correlation with experiments. Aoki et al.[3] found that, at cryogenic temperatures, quasi-isotropic laminates exhibited a large reduction in the transverse mechanical strain ε_2 that initiates microcracking (from 0.702% at room temperature to 0.325% at cryogenic temperatures).

Currently, there is limited information available on the failure characteristics of composite laminates. Uncertainties in the stiffness and strength properties are introduced by the fabrication process, the

Received 30 January 2001; presented as Paper 2001-1327 at the AIAA/ASME/ASCE/AHS/ASC 42nd Structures, Structural Dynamics, and Materials Conference, Seattle, WA, 16–19 April 2001; revision received 23 December 2002; accepted for publication 25 May 2003. Copyright © 2003 by the authors. Published by the American Institute of Aeronautics and Astronautics, Inc., with permission. Copies of this paper may be made for personal or internal use, on condition that the copier pay the $10.00 per-copy fee to the Copyright Clearance Center, Inc., 222 Rosewood Drive, Danvers, MA 01923; include the code 0001-1452/03 $10.00 in correspondence with the CCC.

*Ph.D. Candidate, Department of Mechanical and Aerospace Engineering, P.O. Box 116250; xueyong@mae.ufl.edu.
†Distinguished Professor, Department of Mechanical and Aerospace Engineering, P.O. Box 116250; haftka@ufl.edu. Fellow AIAA.
‡Assistant Professor, Deptartment of Aerospace Engineering and Engineering Mechanics, Mail Code 1308; satchi@engineering.sdsu.edu.
§Aerospace Engineer, Mechanics and Durability Branch, Mail Stop 396; t.f.johnson@larc.nasa.gov.

temperature dependence of material properties, the cure reference temperature, and the acceptable crack density for design. The traditional way to design the laminate deterministically with some safety factors may not work well for this problem due to various uncertainties and the laminate cracking failure mode. These uncertainties indicate a need to use reliability-based optimization to design laminates for use at cryogenic temperatures. The present research identified uncertainty parameters that have the largest influence on the optimum design and quantified the weight penalty associated with level of uncertainty in those parameters. The reliability-based optimization is carried out using response surface approximations combined with Monte Carlo simulation.[5]

Simple analytical models and simplifying assumptions on statistical distributions are employed. These allowed us to assess the utility of various strategies for reducing structural weight. For actual design, however, more accurate models need to be used.

Deterministic Design of Angle-Ply Laminate

The first step to investigate the design problem was to study the deterministic design of the laminate. It is estimated that the minimum thickness needed to prevent hydrogen leakage is 0.04 in. (0.01 m); thus, it may be acceptable to permit matrix cracking if the undamaged part of the laminate has a minimum thickness of 0.04 in. (0.01 m).

Problem Formulation

Laminates with two ply angles, $[\pm\theta_1/\pm\theta_2]_S$ were optimized (Fig. 1). The x direction corresponds to the hoop direction on a cryogenic propellant tank, whereas the y direction corresponds to the axial direction. The laminates are made of IM600/133 graphite–epoxy material with a ply thickness of 0.005 in. (0.000127 m) and subjected to a mechanical load and an operating temperature of −423°F (−252.8°C), where the hoop and axial stress resultants N_x is 4800 lb/in. (8.4×10^5 N/m) and N_y is 2400 lb/in. (4.2×10^5 N/m).

The design problem was formulated as

$$\begin{aligned} &\text{minimize} \quad h = 4(t_1 + t_2) \\ &\text{such that} \\ &\varepsilon_1^l \le \varepsilon_1 \le \varepsilon_1^u \\ &\varepsilon_2^l \le \varepsilon_2 \le \varepsilon_2^u \\ &|\gamma_{12}| \le \gamma_{12}^u \\ &0.005 \le t_1, t_2 \\ &0.040 \le h \end{aligned} \tag{1}$$

where thickness is in inches (meters) and where h is the laminate thickness, superscripts u and l denote upper and lower limits of associated quantities, and ε_1, ε_2, and γ_{12} are the ply strains along fiber direction, transverse to fiber direction, and shear strain, respectively. The stack thickness of plies with ply angle θ_1 and θ_2 are t_1 and t_2, respectively. The four design variables are the ply angles θ_1 and θ_2 and their stack thickness t_1 and t_2. The individual stack thickness from a continuous optimizer (Sequential Quadratic Programming in MATLAB®) is rounded up to the nearest multiple of 0.005 in.

Table 1 shows the strain allowables for the lamina, which are determined from experiments and explained in Appendix A. The strain allowables may appear to be high; however, they are applied to strain

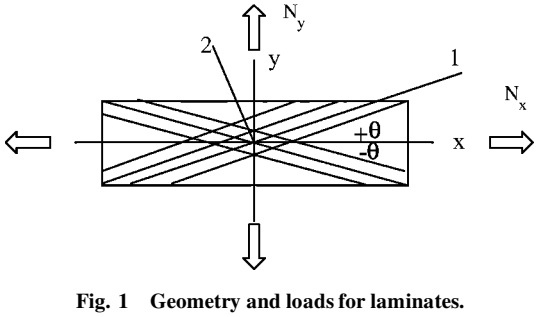

Fig. 1 Geometry and loads for laminates.

Table 1 Strain allowables[a] for IM600/133 at −423°F (−252.8°C)

Strain	Allowables
ε_1^u	0.0103
ε_1^l	−0.0109
ε_2^u	0.0110 or 0.0154[b]
ε_2^l	−0.0130
γ_{12}^u	0.0138

[a]Strain allowables include residual strains calculated from the stress-free temperature of 300°F (148.9°C).
[b]Value 0.0110 is obtained from the extreme value 0.0154 divided by a safety factor of 1.4, as shown in Appendix A.

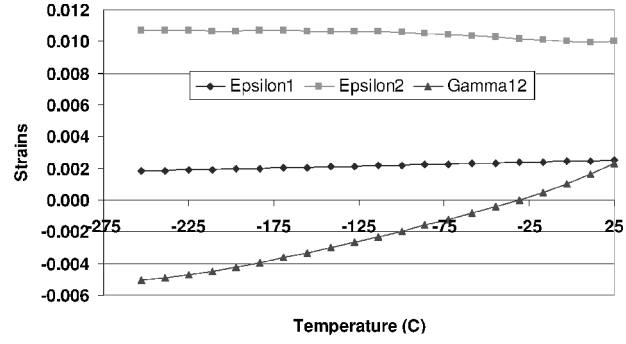

Fig. 2 Strains in optimal laminate for temperature-dependent material properties with $\varepsilon_2^u = 0.0110$ (second design in Table 2).

including residual strains that develop due to cooling from stress-free temperature of 300°F (148.9°C). As shown in Appendix A, a quasi-isotropic laminate will use up its entire transverse strain allowable of 0.011, when cooled to −452°F (−268.9°C). This value is conservative in view of the experiments by Aoki et al.[3] that indicated that the laminate can carry 0.325% mechanical strain at cryogenic temperatures.

The stress-free temperature of IM600/133 is assumed to be 300°F (148.9°C). The material properties of IM600/133 were taken from Aoki et al.[3] Because these properties, such as coefficients of thermal expansion and elastic moduli, change substantially with temperature, classical lamination theory (CLT) with temperature-dependent material properties is applied (see summary in Appendix B). The calculations used smooth polynomials fitted to material properties (figures in Appendix A) using JMP software.[6]

Optimization Results

To see the effect of mechanical and thermal loads, it is instructive to compare designs for different operational temperatures. As shown in Table 2 of Qu et al.,[4] a cross-ply laminate with a thickness of 0.04 in. (0.01 m) can easily (with 0.1% transverse strain as the margin of safety) carry the mechanical loads. When thermal strains are taken into account, the angle between the $\pm\theta$ plies must decrease to reduce the thermal strains. At cryogenic temperatures, the angle decreases to 25.5 deg, and at that angle, the axial loads cannot be carried efficiently and the thickness increases to 0.1 in. (0.00254 m). It is shown in the Fig. 2 of Qu et al.[4] that at −423°F (−252.8°C) the thickness of optimum laminates obtained by using temperature-dependent material properties is 80% less than that using constant material properties at 77°F (25°C). Using temperature-dependent material properties avoided a very conservative design with constant material properties.

Because designs must be feasible for the entire range of temperatures, strain constraints were applied at 21 different temperatures, which were uniformly distributed from 77 to −423°F (−252.8°C). Table 2 shows that the design problem has multiple optima. Figure 2 shows that the tensile strain limit ε_2^u is the active constraint at −423°F (−252.8°C) for the second optimal design in Table 2.

These optimal laminates have similar thicknesses but different ply angles. The failure probabilities of the continuous designs are

Table 2 Optimal laminates for temperature-dependent material properties with ε_2^u of 0.0110 (optimized for 21 temperatures)

θ_1, deg	θ_2, deg	t_1, in. (m)	t_2, in. (m)	h,[a] in. (m)	Probability of failure[b]
0.00	28.16	0.005 (0.000127)	0.020 (0.000508)	0.100 [0.103] (0.00254)	0.019338 (0.014541)
27.04	27.04	0.010 (0.000254)	0.015 (0.000381)	0.100 [0.095] (0.00254)	0.000479 (0.001683)
25.16	27.31	0.005 (0.000127)	0.020 (0.000508)	0.100 [0.094] (0.00254)	0.000592 (0.001879)

[a]Numbers in brackets indicate unrounded thickness.
[b]Numbers in parentheses are for unrounded design. Probabilities were calculated by the methodology described in the next section.

Table 3 Optimal laminates for reduced axial load of 1200 lb/in. (2.1×10^5 N/m) by using load-shunting cables [equivalent laminate thickness of 0.005 in. (0.000127 m)]

θ_1, deg	θ_2, deg	t_1, in. (m)	t_2, in. (m)	h,[a] in. (m)	Probability of failure[b]
0.00	29.48	0.005 (0.000127)	0.005 (0.000127)	0.040 [0.043] (0.001)	0.010311 (0.001156)
27.98	26.20	0.005 (0.000127)	0.005 (0.000127)	0.040 [0.043] (0.001)	0.585732 (0.473536)
30.62	11.31	0.005 (0.000127)	0.005 (0.000127)	0.040 [0.042] (0.001)	0.008501 (0.008363)

[a]Numbers in brackets indicate unrounded thickness.
[b]Numbers in parentheses are for unrounded design. Probabilities were calculated by the methodology described in the next section.

shown in brackets. The high failure probabilities of the first design (continuous and discrete) clearly show a smaller safety margin than the other two. The second and third designs show that a slight rounding can change the failure probability significantly. Designs with two similar ply angles have much lower failure probabilities than designs with two substantially different ply angles. The failure probabilities of these laminates are too high. We expect that requirements will be of the order of 10^{-4}–10^{-6}, and this provides incentives to conduct reliability-based design.

As described by Qu et al.,[4] designs with some matrix cracking, assuming that the undamaged laminate has a thickness of at least 0.04 in. (0.01 m), were performed. However, this did not lead to lighter design.

Optimizations with Reduced Axial Load N_y

With small ply angles, the critical component of the load is the axial load N_y, induced by pressure on the caps of the propellant tank. A smaller axial load may be obtained by using an auxiliary structure to carry part of this load, such as axial stiffeners or a cable connecting the caps. If the auxiliary structure does not directly connect to the wall of the hydrogen tank, for example, attached to the caps of the tank, it will not be affected by the mismatch of the thermal expansion coefficients, that is, the residual thermal strains. Here we explored the possibility of halving the axial load through carrying 1200 lb/in. (2.1×10^5 N/m) of the axial load with a cable made of unidirectional material. The required cross-sectional area of the composite cable is 5.05 in.^{2} (0.0033 m^2), which is equivalent to a laminate thickness of 0.005 in. (0.000127 m) for a tank with a 160-in. (4.064-m) radius. Table 3 lists designs optimized with half of the axial load. The results revealed that reducing axial load is an effective way to reduce the laminate thickness. Higher probabilities of failure reflect a rounding down of the thickness.

Reliability-Based Optimization

Problem Formulation

The reliability-based optimization is formulated as

$$\begin{aligned} &\text{minimize} \quad h = 4(t_1 + t_2) \\ &\text{such that} \\ &\quad P \le P^u \\ &\quad 0.005 \le t_1, t_2 \end{aligned} \tag{2}$$

where h is the laminate thickness, t_1 and t_2 are the stack thicknesses of lamina with ply angles θ_1 and θ_2, respectively. The limits on t_1 and t_2 also ensure that the laminate has a minimum thickness of 0.04 in. (0.01 m) to prevent hydrogen leakage. The reliability constraint is expressed as a limit P^u, that is, $P^u = 10^{-4}$, on the probability of failure, P. The probability of failure is based on first-ply failure according to the maximum strain failure criterion. The four design variables are the ply angles θ_1 and θ_2 and their stack thickness t_1 and t_2.

Table 4 CV of the random variables

Random variables	CV
$E_1, E_2, G_{12}, \mu_{12}$	0.035
α_1, α_2	0.035
T_{zero}	0.030
$\varepsilon_1^u, \varepsilon_1^l$	0.06
$\varepsilon_2^u, \varepsilon_2^l, \gamma_{12}^u$	0.09

The 12 random variables are 4 elastic properties, E_1, E_2, G_{12}, and μ_{12}; two coefficients of thermal expansion, α_1 and α_2; 5 ply strain allowables, ε_1^u, ε_1^l, ε_2^u, ε_2^l, and γ_{12}^u; and the stress-free temperature of the material, T_{zero}. Table 4 shows the coefficients of variation (CV) of the random variables that are assumed to be normally distributed and uncorrelated. Those CVs, which are based on limited test data provided to us by the manufacturers, are intended only for illustration. The mean values of the strain limits are shown in Table 1; ε_2^u is 0.0154. The mean value of the stress-free temperature is assumed as 300°F. The mean values of the other random variables, which change as functions of temperature, are given in Appendix A.

Response Surface Approximations for Reliability-Based Optimization

The limit state function of a reliability analysis problem can be defined as

$$Z = g(\boldsymbol{x}) \tag{3}$$

where Z is a performance criterion and $\boldsymbol{x}$ is the random variable vector. The failure event is defined as $Z < 0$, and the failure surface or limit state of interest can be described as $Z = 0$. The probability of failure can be calculated as

$$P_f = \int_{g(\boldsymbol{x}) < 0} f_X(\boldsymbol{x})\, \mathrm{d}\boldsymbol{x} \tag{4}$$

where $f_X(\boldsymbol{x})$ is the joint probability distribution function. This integral is difficult to evaluate in high dimensions because the domain defined by $g(x) < 0$ is usually unknown.

Commonly used probabilistic design methods are based on either simulation techniques, such as Monte Carlo simulation, or moment-based methods, such as the first-order-reliability method (e.g., Ref. 7). Monte Carlo simulation is easy to implement, robust, and accurate with sufficiently large sample size, but it may require a relatively large number of analyses to obtain a good estimate of failure probability. Monte Carlo simulation, which also produces a noisy response, is difficult to use with gradient-based optimization. Moment-based methods are not well suited for problems with many

competing critical failure modes. Response surface approximations can help solve the two problems of Monte Carlo simulation, namely, simulation cost and noise from random sampling.

Response surface approximations (e.g., Ref. 8) usually fit low-order polynomials to the structural response in terms of random variables

$$\hat{\boldsymbol{g}}(\boldsymbol{x}) = \boldsymbol{X}\boldsymbol{b} \tag{5}$$

where $\hat{\boldsymbol{g}}$ is an $n \times 1$ vector of the responses, $\boldsymbol{X}$ is an $n \times k$ matrix of the levels of the independent variables, and $\boldsymbol{b}$ is a $k \times 1$ vector of the least-square regression coefficients. The polynomial approximation is then used in the place of detailed analyses to reduce the computational cost of probability calculation. The fitted smooth polynomials also filter out noise in response.

Response surface approximations used for reliability-based designs can be implemented in different ways. Qu et al.[5] provides a review of current methods and developed an analysis response surface (ARS) approach. For the present paper, response surfaces of two types were created. The first type is ARS, which is fitted to the strains in the laminate in terms of both design variables and random variables. When the ARS is used, the probability of failure at every design point can be calculated inexpensively by Monte Carlo simulation based on the fitted polynomials. The second type of response surface is design response surface (DRS), which is fitted to probability of failure as a function of design variables. The DRS is created to filter out noise induced by the Monte Carlo simulation and is used to calculate the reliability constraint in the design optimization.

ARS

Besides the design and random variables described in the problem formulation, the service temperature was treated as a variable ranging from 77 to −423°F (25 to 252.8°C) to avoid constructing ARS at each selected temperature. Therefore, the total number of variables was 17. However, the strains in the laminate do not depend on the 5 strain allowables, so that the ARS were fitted to the strains in terms of 12 variables, including 4 design variables, 4 elastic properties, 2 coefficients of thermal expansion, the stress-free temperature, and the service temperature. The range of the design variables (Table 5) for the ARS was chosen based on the values of the optimal deterministic design. Ranges for random variables were automatically handled as explained subsequently. When the ARS and 5 strain allowables were used, probabilities of failure were calculated by Monte Carlo simulations, whereas the strain constraints were evaluated at 21 uniformly distributed service temperatures between 77 and −423°F (25 to −252.8°C).

The accuracy of the ARS is evaluated by statistical measures provided in JMP software,[6] including the adjusted coefficient of multiple determination, R^2_{adj}, and the rms error predictor. To improve the accuracy of response surface approximation, polynomial coefficients that were not well characterized were eliminated from the response surface model by using a mixed stepwise regression (e.g., Ref. 9).

Table 5 Range of design variables for analysis response surfaces

Design variable	Range
θ_1, deg	20–30
θ_2, deg	20–30
t_1, in. (m)	0.0125–0.03 (0.000318–0.000762)
t_2, in. (m)	0.0125–0.03 (0.000318–0.000762)

Table 6 Quadratic analysis response surfaces of strains (millistrain)

	Analysis response surfaces based on 182 LHS points					
Error statistics	ε_1 in θ_1	ε_2 in θ_1	γ_{12} in θ_1	ε_1 in θ_2	ε_2 in θ_2	γ_{12} in θ_2
R^2_{adj}	0.9977	0.9956	0.9991	0.9978	0.9961	0.9990
RMS error predictor	0.017	0.060	0.055	0.017	0.055	0.060
Mean of response	1.114	8.322	−3.13	1.108	8.328	−3.14

Table 7 Design response surfaces for probability of failure[a]

Error statistics	FCCCD 25 points (quadratic)	LHS 252 points (fifth order)	LHS 252 points + FCCCD 25 points (fifth order)
R^2_{adj}	0.6855	0.9926	0.9982
RMS error predictor	0.00053	0.000003	0.000012
Mean of response	0.00032	0.000016	0.000044

[a]Probability calculated by MCS with a sample size of 1,000,000.

The statistical design of experiment of ARS was Latin hypercube sampling or Latin hypercube design [(LHS), e.g., Ref. 10], where design variables were treated as uniformly distributed variables to generate design points. LHS is more flexible than standard orthogonal arrays, because LHS can generate an arbitrary number of samples. LHS provides a very good design of experiments for random variables, by sampling each variable according to its probability distribution and, therefore, determining the range of random variables for ARS. The efficiency of LHS was demonstrated in the work of Qu et al.[5] Face center central composite design [(FCCCD), e.g., Ref. 9] and LHS were employed to construct DRS.

Because the laminate has two ply angles and each ply has three strains, six ARS were needed in the optimization. A quadratic polynomial of 12 variables has 91 coefficients. The number of sampling points generated by LHS was selected to be twice the number of coefficients. Table 6 shows that the quadratic response surfaces constructed from LHS, with 182 points, offer good accuracy.

DRS

The six quadratic ARS were used to calculate the probabilities of failure with Monte Carlo simulation. Because the fitting errors in DRS are generally larger than the random errors from finite sampling in probability calculation,[5] Monte Carlo simulation only needs to be performed until relatively small confidence intervals are achieved. Therefore, a sample size of 1,000,000 was employed. The design points of DRS combine FCCCD and LHS. Table 7 shows a comparison of the three DRS. The accuracy of the quadratic response surface is unacceptable. The accuracy of fifth-order response surface (with 126 unknown coefficients before stepwise regression) was improved by using a reciprocal transformation on the thicknesses t_1 and t_2 because the probability of failure, like most structural responses, is inversely correlated with the stack thickness. We found that LHS might fail to sample points near some corners of the design space, leading to poor accuracy around these corners. We, therefore, combined LHS with FCCCD, which includes all of the vertices of the design space. The accuracy of DRS based on LHS combined with FCCCD is slightly worse than DRS based on LHS alone because the probabilities at the corners of the design space are usually extremely low or high, presenting a greater fitting difficulty than without FCCCD. However, the extrapolation problem was solved, and the side constraints are set as the range of the ARS shown in Table 5. The error of 0.000012 is much lower than the allowable failure probability of 0.0001.

Reliability-Based Designs

Table 8 shows a comparison of the reliability-based optimum with the three deterministic optima from Table 2 and their failure probabilities. The optimal thickness increased from 0.100 to 0.120 in. (0.00254 to 0.003 m), whereas the failure probability decreased by about one order of magnitude.

The reliability-based designs in Table 8 show that ply angles close to 25 deg offer designs with low failure probability. Furthermore, good designs require only a single ply angle, which allows simplification of the configuration of the laminate from $[\pm\theta_1/\pm\theta_2]_S$ to $[\pm\theta]_S$. Table 9 shows the failure probabilities of some chosen designs calculated with Monte Carlo simulation (MCS) using ARS. The laminates with ply angles of 24, 25, and 26 deg offer lower

Table 8 Comparison of reliability-based optimum with deterministic optima

Optimal design $[\theta_1, \theta_2$, deg; t_1, t_2, in.]	Laminate thickness, in. (m)	Failure probability from MCS of ARS 1,000,000 samples	Allowable probability of failure
[24.89, 25.16; 0.015, 0.015]	0.120 [0.120][a] (0.003)	0.000055	0.0001
[0.00, 28.16; 0.005, 0.020]	0.100 [0.103] (0.00254)	0.019338[b]	
[27.04, 27.04; 0.010, 0.015]	0.100 [0.095] (0.000254)	0.000479	Deterministic optima
[25.16, 27.31; 0.005, 0.020]	0.100 [0.094] (0.00254)	0.000592	

[a]The numbers in the brackets indicate unrounded thickness.
[b]This deterministic optimum is out of the range of ARS; probability of failure calculated by MCS based on another set of ARS.

Table 9 Refined reliability-based design[a] with a thickness of 0.12 in., $[\pm\theta]_S$

θ, deg	Probability of failure
23.0	0.0000718
24.0	0.0000605
25.0	0.0000565
26.0	0.0000607
27.0	0.0000792

[a]MCS with a sample size of 10,000,000.

Table 10 Comparison of probability of failure from MCS-based ARS and CLT[a]

Sample	Number of samples	Failure probability
ARS	1×10^7	0.0000565
CLT	1×10^6	0.000069

[a]Optimal design θ_1 and $\theta_2 = 25$ deg and t_1 and $t_2 = 0.015$ in. (0.000381 m) and laminate thickness 0.120 in. (0.003 m).

Table 11 Accuracy of Monte Carlo simulation

Monte Carlo simulation	Coefficient of variation, %	Percentage errors (absolute errors) for 95% confidence interval
1×10^7 samples	4.2	8.4% ($\pm 4.75 \times 10^{-6}$)
1×10^6 samples	12.05	24.1% ($\pm 1.66 \times 10^{-5}$)

probabilities of failure than the others. These three laminates will be studied further.

Quantifying Errors in Reliability Analysis

The reliability analysis has errors due to MCS with limited sample size and due to the approximation of CLT analysis by analysis response surface approximations. To evaluate the magnitude of errors in reliability analysis, the probability of failure of the rounded design was evaluated by using MCS with the exact analysis (CLT), but only 1,000,000 analyses were performed due to the cost of computation. Table 10 shows a comparison of the results of MCS based on ARS and that based on CLT. The difference is approximately 1.25×10^{-5}.

When each simulation is assumed to have a Bernoulli trial and the N trials are assumed to have binomial distribution, the CV of the probability obtained by MCS can be estimated, as well as the percentage error corresponding 95% confidence interval (e.g., Haldar and Mahadevan[11]). Table 11 shows the accuracy and error bounds for MCS. Together with Table 10, the error calculation indicates that the probability of failure of the rounded design is still below the target probability of failure of 0.0001. The errors can be reduced by more accurate approximations and advanced MCS. Another reliability-based design cycle in a reduced-size design region can be performed to be more accurate.

Effects of Quality Control on Laminate Design

When deterministic designs are compared to the reliability-based design, there is an increase of 20% in the thickness. In addition, the design failure probability of 10^{-4} is quite high. To improve the design, the possibility of limiting the variability in material properties through quality control (QC) is considered. Here, QC means that materials are tested by the manufacturer and/or fabricator; extremely poor batches are not accepted. Normal distributions assume the possibility (however small) of unbounded variation. In practice, QC truncates the low end of the distribution. Specimens with extremely poor properties are rejected. It is also assumed that specimens with exceptional properties are scarcer than those with poor properties. The normal distribution will be truncated on the high side at 3σ (excluding 14 out of 10,000 specimens) and on the low side at different values corresponding to different levels of QC. The tradeoff between QC, failure probability, and laminate thickness (weight) will be explored.

Table 12 Effects of QC of ε_2^u on probability of failure for $(\pm\theta)_S$ 0.12-in.-thick laminates

θ, deg	Probability of failure[a]			
	Untruncated normal	Truncate at -4σ (3/100,000)	Truncate at -3σ (14/10,000)	Truncate at -2σ (23/1000)
24.0	60.5×10^{-6}	30.5×10^{-6}	0.0	0.0
25.0	56.5×10^{-6}	29.9×10^{-6}	0.1×10^{-6}	0.0
26.0	60.7×10^{-6}	31.0×10^{-6}	0.5×10^{-6}	0.0

[a]From MCS 10,000,000 samples.

Because the primary failure mode of the laminate is microcracking, the tensile strain limit ε_2^u is the first quantity to be improved by QC. The normal distribution of ε_2^u is truncated at 3σ to exclude unrealistically strong specimens. On the low side, QC at -4σ, -3σ, and -2σ was checked; this corresponds to rejecting 3 specimens of 100,000; 14 specimens of 10,000; and 23 specimens of 1000; respectively. Table 12 shows the change in the failure probability for selected reliability-based designs. QC on ε_2^u is a very effective way to reduce the probability of failure. A relatively low cost QC of ε_2^u at 3σ will reduce the failure probability by more than two orders of magnitude. As shown in Tables 15 and 16 of Qu et al.,[4] QC on other allowables, elastic properties, and coefficients of thermal expansion was found to have very limited influence on the probability of failure. Therefore, the primary failure mode of the laminate is microcracking, and ε_2^u is the critical parameter to study further.

Instead of reducing failure probability, QC can be used to reduce the laminate thickness. Table 13 shows that QC of ε_2^u at -2.8σ will allow 0.1-in. (0.0254-m)-thick laminates with failure probability below the required 0.0001. QC of ε_2^u at -1.3σ, which corresponds to rejecting 97 specimens out of 1000, will reduce the thickness to 0.08 in. (0.002 m).

Effects of Other Improvements to Material Properties

Instead of QC, it is possible to improve the design by using a better material. Table 14 shows the effects of changing the mean value of ε_2^u by $\pm 10\%$ of the nominal value of 0.0154. Comparison with Table 12 shows that a 10% improvement has a big influence on failure probability but is not as powerful as QC at -3σ level.

The failure probability also depends on the CV of ε_2^u. The CV can be improved if the manufacturing can be more consistent. Table 15 shows that the failure probabilities are not as sensitive to changes in the CV as to changes in the mean value of ε_2^u, but 10% reduction in the CV can still reduce the failure probability by about a factor of five.

Table 13 Effects of QC of ε_2^u on probability of failure for $(\pm 25)_S$ deg laminates of different thicknesses

	Probability of failure[a]			
h, in. (m)	Untruncated normal	Truncate at -3σ (14/10,000)	Truncate at -2.8σ (26/10,000)	Truncate at -1.3σ (97/1000)
0.08 (0.002)	0.028289	0.027103	0.026145	0.000068
0.10 (0.00254)	0.001030	0.000229	0.000088	0.0
0.12 (0.003)	0.000057	0.0	0.0	0.0

[a]From MCS 10,000,000 samples.

Table 14 Sensitivity of failure probability to mean value of ε_2^u (CV = 0.09) for $(\pm\theta)_S$ 0.12 in. (0.003 m)-thick laminates[a]

$E(\varepsilon_2^u)$	Probability of failure[b]
0.0154	56.5×10^{-6}
0.01694	3.4×10^{-6}
0.01386	996.7×10^{-6}

[a]Here, $\theta = 25.0$ deg. [b]From MCS 10,000,000 samples.

Table 15 Sensitivity of failure probability to CV of $\varepsilon_2^u[E(\varepsilon_2^u) = 0.0154]$ for $(\pm\theta)_S$ 0.12 in. (0.003 m)-thick laminates[a]

CV	Probability of failure[b]
0.09	56.5×10^{-6}
0.099	208.2×10^{-6}
0.081	10.8×10^{-6}

[a]Here, $\theta = 25.0$ deg. [b]From MCS 10,000,000 samples.

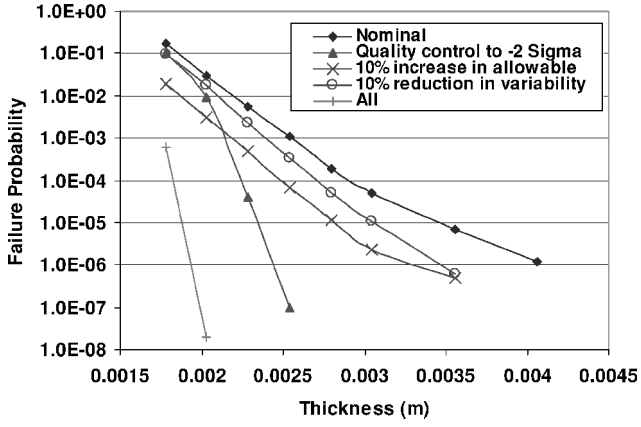

Fig. 3 Tradeoff of probability of failure, cost, and weight (laminate thickness) for $[\pm 25]_S$.

Figure 3 combines several effects discussed earlier to show a tradeoff plot of probability of failure, cost (truncating and changing the distribution of ε_2^u), and weight (thickness) for a laminate of $[\pm 25]_S$. For a probability of failure less than 1×10^{-3}, QC at the -2σ level is more effective for reducing the probability of failure than increasing the mean value by 10% or decreasing the CV by 10%. The reason is that small failure probability is heavily affected by the tails of the distributions. For large failure probability, increasing the mean value of ε_2^u is more effective. Increasing the mean value of ε_2^u by 10% or truncating ε_2^u at -2σ can reduce the laminate thickness to 0.10 in. (0.00254 m) for a safety level of 1×10^{-4}. When all three measures are combined together, the laminate thickness can be reduced to 0.08 in. with a safety level of 1×10^{-7}.

Table 16 shows the changes of maximum ε_2 calculated by the laminate analyses. Changes of 10% of the mean values of E_2, T_{zero}, and α_2 (same CV) will lead to approximately 5% change in the maximum ε_2, which indicates that further study needs to focus on the three quantities. Table 17 shows that the probabilities of failure are reduced by a factor of five by a 10% change of the mean values of E_2, T_{zero}, and α_2 (same CVs). This reduction of probability shows the potential of further improvements via improvements in all three material properties.

Table 16 Maximum ε_2 (millistrain)[a] induced by the change of material properties E_1, E_2, G_{12}, μ_{12}, T_{zero}, α_1, and α_2 for $[\pm 25]_S$ deg 0.12-in.-thick laminate

Nominal maximum $\varepsilon_2 = 9.859$	Maximum ε_2						
	E_1	E_2	G_{12}	μ_{12}	T_{zero}	α_1	α_2
$0.9 \times$ nominal	9.901	10.469	9.763	9.909	9.320 (5.47%)	9.857	9.399 (4.67%)
$1.1 \times$ nominal	9.824	9.313 (5.54%)	9.960	9.981	10.584	9.861	10.333

[a]From deterministic analyses for 21 temperature.

Table 17 Probability of failure for $[\pm 25]_S$ deg 0.12 in.-thick laminate with improved average material properties[a]

Measure	Probability of failure
Nominal	0.0000565
$1.1 \times E(E_2)$	0.0000117
$0.9 \times E(T_{\text{zero}})$	0.0000116
$0.9 \times E(\alpha_2)$	0.0000110
All three	0.0000003

[a]Monte Carlo simulation with a sample size of 10,000,000.

Conclusions

The design of hydrogen tanks for cryogenic environments poses a challenge because of large thermal strains that can cause matrix cracking, which may lead to hydrogen leakage. The laminate design must use ply angles that are not too far apart to reduce the thermal residual strains, compromising the ability of the laminate to carry loads in two directions. These small ply angles can cause the laminate thickness to more than double compared to what is needed to carry only the mechanical loads in the application study here.

Various solutions for alleviating this problem were evaluated. First, deterministic optimizations showed that allowing microcracking in part of the laminate does not help, but shunting part of the load to an auxiliary structure, such as a cable connecting the two caps, may be a reasonable approach. The high probabilities of failure of deterministic designs motivate reliability-based design.

Reducing the probability of failure required increases in thickness. The most influential uncertainty was variability in the tensile strain allowable in the direction transverse to the fibers, ε_2^u. Limiting this variability can reduce the required thickness. Of the different options studied in the paper, QC on the transverse tensile allowable, ε_2^u, proved to be the most effective option. QC at the -1.3σ level of ε_2^u, corresponding to a rejection of about 9.7% of the specimens, can reduce the required thickness by one-third. Reductions in the CV of ε_2^u, or an increase in its mean value, also reduces the failure probability substantially. Increasing the transverse modulus E_2, decreasing the coefficient of thermal expansion α_2, and reducing the stress-free temperature T_{zero} can also help considerably.

Appendix A: Determination of Strain Limit Corresponding to Onset of Matrix Cracking

The material properties of IM600/133 were taken from Aoki et al.[3] and fitted with smooth polynomials to be used in calculations. Figures A1 and A2 show curves of material properties to temperatures. Data from Aoki et al.[3] were used to determine the strain allowables. They tested a 16-ply quasi-isotropic $(45/0/-45/90)_{2s}$ symmetric laminate in tension in the 0-deg direction at cryogenic temperatures. The nominal specimen thickness and width were 2.2 mm and 15 mm. The mechanical loads corresponding to matrix cracks (Table A1) were extracted from Fig. 5 by Aoki et al.[3] The strain transverse to the fiber direction, ε_2, is assumed to be the strain that induces matrix cracking in the laminate. Based on the load condition and the configuration of the laminate, the transverse strain ε_2 in the 90-deg plies is the most critical strain in the laminate.

Normally, strain allowables are calculated by loading laminates at room temperatures. However, for microcracking, the residual stresses are of primary importance, and so all strains are calculated from the stress-free temperature, assumed to be 300°F. The calculations are made by integrating the thermal strains from the stress-free temperature to the operational temperature as described in Appendix B.

Table A1 Transverse strains corresponding to the onset of matrix cracking in the 90-deg piles of a quasi-isotropic $(45/0/-45/90)_{2s}$

Quantity	Room temperature (77°F or 25°C)	LN_2 temperature (−320°F or −196°C)	LHe temperature (−452°F or −269°C)	LHe temperature (−452°F or −269°C)[a]
Mechanical load, MPa	390	330	200	50[a]
Total ε_2	0.01564	0.01909	0.01760	0.01517[a]
Thermal ε_2	0.00864	0.01365	0.01435	0.01435[a]
Mechanical ε_2	0.00700	0.00544	0.00325	0.00082[a]

[a]Older data obtained from Aoki et al.[12]

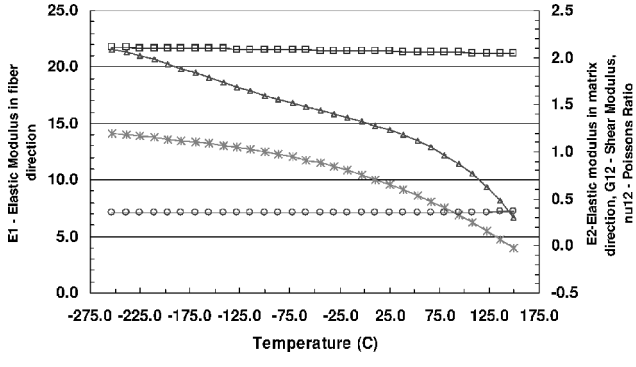

Fig. A1 Polynomials fit to elastic properties: □, E_1 (Mpsi); △, E_2 (Mpsi); ∗, G_{12} (Mpsi); and ○, μ_{12}.

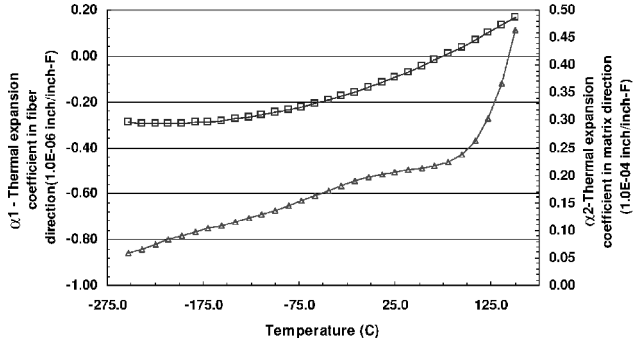

Fig. A2 Polynomials fit to coefficient of thermal expansion: □, α_1 and △, α_2.

Table A2 Transverse strains of an angle-ply laminate $(\pm 25)_{4s}$ under the same loading condition as Table A1

Quantity	Room temperature (77°F or 25°C)	LN_2 temperature (−320°F or −196°C)	LHe temperature (−452°F or −269°C)	LHe temperature (−452°F or −269°C)[a]
Mechanical load, MPa	390	330	200	50[a]
Total ε_2	−0.00261	0.00360	0.00527	0.00656[a]
Thermal ε_2	0.00393	0.00669	0.00699	0.00699[a]
Mechanical ε_2	−0.00654	−0.00309	−0.00172	−0.00043[a]

[a]Older data obtained from Aoki et al.[12]

Table A1 shows the transverse strains ε_2 in the 90-deg plies corresponding to the loading at the onset of matrix cracking at selected temperatures. Aoki et al.[3] found that the maximum mechanical strain before matrix cracking is reduced from 0.7% at room temperature to 0.325% at −452°F (−268.9°C). Earlier results from 1999,[12] also given in Table A1, indicated that the maximum mechanical strain at cryogenic temperatures may be as low as 0.082%. However, the calculation indicates that the total strain (including the residual thermal strain) may vary anywhere from 1.5 to 1.9% depending on the temperature and the measurement. These values appear high, but this is because they include the residual strains that are usually not counted. For the quasi-isotropic laminate, these residual strains at room temperature are very high (at 0.86%) and are higher at lower temperatures.

The importance of working with strains measured from the stress-free temperature is demonstrated in Table A2, which shows the ε_2 in the angle-ply laminate $(\pm 25)_{4S}$ under the same loading condition as Table A1. At room temperature, the residual (thermal) strains are only about 0.4% compared to 0.86% for the quasi-isotropic laminate. An analysis based on strains measured from room temperature will not show the additional 0.46% strain that the $(\pm 25)_{4S}$ laminate can carry compared to a quasi-isotropic laminate. Based on the data from Table A1, we selected the allowable strain to be 1.54% for the probabilistic design and 1.1% (1.4 safety factor) for the deterministic design.

Appendix B: Composite Laminates Analysis Under Thermal and Mechanical Load

In this section, CLT (e.g., Ref. 13) is modified to take account of temperature-dependent material properties. The stress-free strain of a lamina is defined as $\varepsilon^F = \alpha \Delta T$, where α is the coefficient of thermal expansion. When α is a function of temperature T, the stress-free strain is given by the expression

$$\varepsilon^F = \int_{T_{\text{zero}}}^{T_{\text{service}}} \alpha(T)\, \mathrm{d}T \tag{B1}$$

where T_{zero} is the stress-free temperature of the material and T_{service} is the service temperature. From the equilibrium equation and vanishing of residual stress resultant, the equilibrium of a symmetric laminate subjected to pure thermal load with uniform temperature profile through the thickness can be expressed by

$$\boldsymbol{A}(T)\varepsilon^{0N} = \int_{-h/2}^{h/2} \bar{\boldsymbol{Q}}(T)\varepsilon^F \,\mathrm{d}z = \boldsymbol{N}^N(T) \tag{B2}$$

where ε^{0N} is the nonmechanical strain induced by thermal load. The right-hand side of Eq. (B2) is defined as thermal load N^N. From Eq. (B2), the nonmechanical strain induced by thermal load can be expressed by

$$\varepsilon^{0N}(T) = \boldsymbol{A}^{-1}(T)\boldsymbol{N}^N(T) \tag{B3}$$

The residual thermal stress is given by the constitutive equation

$$\boldsymbol{\sigma}^R(T) = \bar{\boldsymbol{Q}}(T)[\varepsilon^{0N}(T) - \varepsilon^F(T)] \tag{B4}$$

The mechanical strain is expressed by

$$\varepsilon^M(T) = \boldsymbol{A}^{-1}(T)\boldsymbol{N}^M(T) \tag{B5}$$

Therefore, the mechanical stress is given by

$$\boldsymbol{\sigma}^M(T) = \bar{\boldsymbol{Q}}(T)\varepsilon^M(T) \tag{B6}$$

By the principle of superposition, the residual strain and total stress in the laminate are expressed by

$$\varepsilon^{\text{residual}}(T) = \varepsilon^M(T) + \varepsilon^{0N}(T) - \varepsilon^F(T) \tag{B7}$$

$$\boldsymbol{\sigma}^{\text{total}}(T) = \boldsymbol{\sigma}^R(T) + \boldsymbol{\sigma}^M(T) \tag{B8}$$

Acknowledgments

This work was supported in part by Grant NAG-1-2177 and Contract L-9889 from NASA Langley Research Center and National Science Foundation Grant DM5-9979711.

References

[1]Park, C. H., and McManus, H. L., "Thermally Induced Damage in Composite Laminates: Predictive Methodology and Experimental Investigation," *Composites Science and Technology*, Vol. 56, 1996, pp. 1209–1219.

[2]Kwon, Y. W., and Berner, J. M., "Matrix Damage of Fibrous Composites: Effects of Thermal Residual Stresses and Layer Sequences," *Computers and Structures*, Vol. 64, No. 1–4, 1997, pp. 375–382.

[3]Aoki, T., Ishikawa, T., Kumazawa, H., and Morino, Y., "Mechanical Performance of CF/Polymer Composite Laminates Under Cryogenic Conditions," AIAA Paper 2000-1605, April 2000.

[4]Qu, X., Venkataraman, S., Haftka, R. T., and Johnson, T. F., "Reliability, Weight, and Cost Tradeoffs in the Design of Composite Laminates for Cryogenic Environments," AIAA Paper 2001-1327, April 2001.

[5]Qu, X., Venkataraman, S., Haftka, R. T., and Johnson, T. F., "Response Surface Options for Reliability-based Optimization of Composite Laminate," 8th American Society of Civil Engineers Specialty Conference on Probabilistic Mechanics and Structural Reliability, PMC Paper 2000-131, July 2000.

[6]*JMP Statistics and Graphics Guide Version 4.0*, SAS Inst. Inc., Cary, NC, 2000.

[7]Melchers, R. E., *Structural Reliability Analysis and Prediction*, Wiley, New York, 1999, Chaps. 3 and 4.

[8]Khuri, A. I., and Cornell, J. A., *Response Surfaces: Designs and Analyses*, 2nd ed., Marcel Dekker, New York, 1996, Chaps. 2–6.

[9]Myers, H. R., and Montgomery, D. C., *Response Surface Methodology*, Wiley, New York, 1995, pp. 312–314.

[10]Wyss, G. D., and Jorgensen, K. H., "A User's Guide to LHS-Sandia's Latin Hypercube Sampling Software," Sandia National Labs., Rept. SAND98-0210, Albuquerque, NM, 1998.

[11]Haldar, A., and Mahadevan, S., *Reliability Assessment Using Stochastic Finite Element Analysis*, Wiley, New York, 2000, pp. 114–116.

[12]Aoki, T., Ishikawa, T., Kumazawa, H., and Morino, Y., "Mechanical Behavior of CF/Polymer Composite Laminates under Cryogenic Environment," 12th International Conference on Composite Materials (ICCM-12), Paper No. 172, Paris, July 1999.

[13]Gürdal, Z., Haftka, R. T., and Hajela, P., *Design and Optimization of Laminated Composite Materials*, Wiley, New York, 1999, Chap. 2.

E. R. Johnson
Associate Editor